



Published in final edited form as:

Circ Res. 2012 September 14; 111(7): 863–875. doi:10.1161/CIRCRESAHA.112.266585.

Mitofusin 2-containing Mitochondrial-Reticular Microdomains Direct Rapid Cardiomyocyte Bioenergetic Responses via Inter-Organellar Ca²⁺ Crosstalk

Yun Chen¹, György Csordás², Casey Jowdy¹, Timothy G. Schneider², Norbert Csordás², Wei Wang³, Yingqiu Liu¹, Michael Kohlhaas⁴, Maxie Meiser⁴, Stefanie Bergem⁴, Jeanne M. Nerbonne³, Gerald W. Dorn II¹, and Christoph Maack⁴

¹Center for Pharmacogenomics, Department of Internal Medicine, Washington University School of Medicine, St. Louis, MO 63110, USA

²Department of Pathology, Anatomy and Cell Biology, Thomas Jefferson University, Philadelphia, PA 19107

³Department of Developmental Biology, Washington University School of Medicine, St. Louis, MO 63110, USA

⁴Klinik für Innere Medizin III, Universitätsklinikum des Saarlandes, 66421 Homburg, Germany

Abstract

Rationale—Mitochondrial Ca²⁺ uptake is essential for the bioenergetic feedback response through stimulation of Krebs cycle dehydrogenases. Close association of mitochondria to the sarcoplasmic reticulum (SR) may explain efficient mitochondrial Ca²⁺ uptake despite low Ca²⁺ affinity of the mitochondrial Ca²⁺ uniporter. However, the existence of such mitochondrial Ca²⁺ microdomains and their functional role are presently unresolved. Mitofusin (Mfn) 1 and 2 mediate mitochondrial outer membrane fusion, while Mfn2, but not Mfn1, tethers endoplasmic reticulum to mitochondria in non-cardiac cells.

Objective—To elucidate roles for Mfn1 and 2 in SR-mitochondrial tethering, Ca²⁺ signaling and bioenergetic regulation in cardiac myocytes.

Methods and Results—Fruit fly heart tubes deficient of the *Drosophila* Mfn ortholog, MARF, had increased contraction-associated and caffeine-sensitive Ca²⁺ release, suggesting a role for Mfn in SR Ca²⁺ handling. While cardiac-specific Mfn1 ablation had no effects on murine heart function or Ca²⁺ cycling, Mfn2 deficiency decreased cardiomyocyte SR-mitochondrial contact length by 30% and reduced the content of SR-associated proteins in mitochondria-associated membranes. This was associated with decreased mitochondrial Ca²⁺ uptake (despite unchanged mitochondrial membrane potential) but increased steady-state and caffeine-induced SR Ca²⁺ release. Accordingly, Ca²⁺-induced stimulation of Krebs cycle dehydrogenases during β-

Address correspondence to: Dr. Christoph Maack, Klinik für Innere Medizin III, Universitätsklinikum des Saarlandes, 66421 Homburg, Germany, Phone: +49-(0)6841-162-1380, FAX: +49-(0)6841-162-3434, christoph.maack@uks.eu, Dr. Gerald W Dorn II, Washington University Center for Pharmacogenomics, 660 S. Euclid Ave., Campus Box 8220, St. Louis, MO 63110. Phone: 314-362-4892, FAX: 314-362-8844, gdorn@dom.wustl.edu.

Publisher's Disclaimer: This is a PDF file of an unedited manuscript that has been accepted for publication. As a service to our customers we are providing this early version of the manuscript. The manuscript will undergo copyediting, typesetting, and review of the resulting proof before it is published in its final citable form. Please note that during the production process errors may be discovered which could affect the content, and all legal disclaimers that apply to the journal pertain.

DISCLOSURES

None.

adrenergic stimulation was hampered in Mfn2-, but not Mfn1-KO myocytes, evidenced by oxidation of the redox states of NAD(P)H/NAD(P)⁺ and FADH₂/FAD.

Conclusions—Physical tethering of SR and mitochondria via Mfn2 is essential for normal inter-organelle Ca²⁺ signaling in the myocardium, consistent with a requirement for SR-mitochondrial Ca²⁺ signaling through microdomains in the cardiomyocyte bioenergetic feedback response to physiological stress.

Keywords

calcium signaling; cardiac metabolism; excitation-contraction coupling; mitochondria; redox

INTRODUCTION

Morphology and function of mitochondria are dynamically regulated through exchange of organelle contents via cycles of fusion and division.¹ The central components of the mitochondrial fusion machinery are evolutionarily conserved, and genetic defects in fusion proteins are a cause of heritable human neurological and ocular diseases.² Because mitochondria are double membrane-bound organelles, content exchange requires fusion of the outer and inner membranes. Experimental manipulation of outer mitochondrial membrane mitofusin (Mfn) 1 and 2 in cultured murine fibroblasts, cerebellum and skeletal muscle has revealed largely overlapping functions for these proteins in tethering mitochondrial outer membranes and inducing organelle fusion.^{3–5}

The heart has a very high energy demand to fuel the ATP-dependent processes of excitation-contraction (EC) coupling.^{6,7} ATP is replenished primarily in mitochondria by oxidative phosphorylation, where the Krebs cycle produces NADH and FADH₂ that fuel the electron transport chain (ETC). This electron flux generates the mitochondrial membrane potential ($\Delta\Psi_m$) which is the driving force for ATP production at the F₁F₀-ATPase, but also for Ca²⁺ uptake into mitochondria via the mitochondrial Ca²⁺ uniporter (MCU). Ca²⁺ is a key regulator of oxidative phosphorylation by stimulating rate-limiting enzymes of the Krebs cycle, increasing the availability of NADH and FADH₂ for the electron transport chain.^{6,7} Yet, the role of mitochondrial fusion proteins in cardiac homeostasis is currently unresolved because the highly ordered subcellular architecture of cardiac myocytes physically enforces inter-mitochondrial connectivity, which may obviate the need for molecular tethering.⁸ Recent studies suggest that mitochondrial fusion and fission occur in the heart,⁹ and essential roles for mitochondrial fusion with functional overlap of Mfn1 and Mfn2 have been described in mitochondrial assembly regulatory factor (MARF) RNAi *Drosophila* heart tubes and in *mfn1/mfn2* double cardiac-specific knockout murine hearts.^{10,11}

The conventional view that mammalian Mfn1 and Mfn2 are largely functionally redundant has been challenged by de Brito and Scorrano's discovery that Mfn2, but not Mfn1, bridges mitochondria and endoplasmic reticulum (ER).¹² Tethering of ER to mitochondria is thought to maintain close associations between the organelles and facilitate local Ca²⁺ delivery to the mitochondrial matrix,¹³ promoting mitochondrial Ca²⁺ signaling.¹⁴ Consistent with Mfn2 functioning as the ER-mitochondrial tether, ablation or suppression of Mfn2 (but not Mfn1) in murine embryonic fibroblasts and HeLa cells increased the spatial separation between ER and mitochondria, augmented ER Ca²⁺ content, and decreased mitochondrial Ca²⁺ uptake after inositol-trisphosphate (IP₃) stimulation. These results established the molecular components of conceptual ER-mitochondrial Ca²⁺ microdomains originally proposed by Rizzuto and Pozzan.¹⁴

In contrast to non-cardiac cells, in which the concept of mitochondrial Ca²⁺ microdomains is now well established,¹⁴ their existence and functional implications in cardiac myocytes are

still unclear.^{7,15–17} In this context, a recent report from Papanicolaou et al calls into question de Brito and Scorrano's findings as they apply to cardiac myocytes.¹⁸ Cardiac-specific ablation of *mfn2* induced mitochondrial enlargement and cardiac hypertrophy in otherwise normal hearts without apparently altering the interaction between mitochondria and sarcoplasmic reticulum (SR) or affecting cardiomyocyte Ca^{2+} cycling.¹⁸ Although Mfn2 deficiency in this study protected cardiomyocytes against mitochondrial depolarization and programmed cell death induced by reactive oxygen species (ROS) as predicted by de Brito and Scorrano,¹² this was attributed to an intrinsic increase in mitochondrial Ca^{2+} retention capacity and decreased sensitivity of the mitochondrial permeability transition pore, but not to altered mitochondrial-SR interactions.¹⁸ The differences between de Brito and Scorrano's findings in fibroblasts¹² and those of Papanicolaou et al in mouse hearts¹⁸ suggest several possibilities: *First*, SR-mitochondrial bridges in cardiac myocytes are not created by Mfn2, but consist of other protein tethers such as PACS-2 and/or IP₃ receptor-VDAC complexes.^{19,20} *Second*, Mfn2 can bridge cardiac myocyte SR and mitochondria, but this physical tethering is functionally unimportant either because of enforced proximity of these organelles in cardiac cells, or because mitochondrial sensing of SR Ca^{2+} released through ryanodine receptors (RyRs) differs from that released via IP₃ receptors.²¹ *Finally*, Mfn2 SR-mitochondrial bridges may exist in cardiac myocytes to serve the purely pathological function described by Papanicolaou et al,¹⁸ increasing mitochondrial sensitivity to Ca^{2+} -mediated depolarization and cell death without altering normal SR or mitochondrial Ca^{2+} handling.

Here, we address these possibilities using a previously described cardiac-specific *Drosophila* MARF (the *Drosophila* mitofusin ortholog) RNAi model¹⁰ and novel murine Mfn1 and Mfn2 knockout models in which mitofusin ablation is induced after birth without confounding toxic effects of the highly expressed Cre transgene used by Papanicolaou et al.²² Our results are consistent with the idea that Mfn2 is an essential component of the physical connections linking mouse cardiomyocyte SR and mitochondria. Disruption of these inter-organelle tethers by Mfn2 ablation slightly increased caffeine-induced SR Ca^{2+} release and steady-state cytosolic Ca^{2+} transients. By simultaneously assaying mitochondrial ($[\text{Ca}^{2+}]_m$) and cytosolic Ca^{2+} ($[\text{Ca}^{2+}]_c$) in “beating” cardiac myocytes and monitoring substrates for oxidative phosphorylation, we further show that interrupting SR-mitochondrial Ca^{2+} cross-talk depresses mitochondrial Ca^{2+} and bioenergetic responses to increased work. Thus, we conclude that Mfn2 is an essential component of cardiomyocyte SR-mitochondrial contact points, and that Ca^{2+} microdomains maintained by Mfn2-mediated SR-mitochondrial tethering are required in the heart to acutely adjust mitochondrial bioenergetic activity to instantaneous metabolic demand.

MATERIALS AND METHODS

Mouse generation and phenotypic analyses

Mfn1^{loxp/loxp} and Mfn2^{loxp/loxp} mice^{4,23} were obtained from University of California-Davis and crossed onto the *Myh6*-nuclear-directed “turbo” Cre line²⁴ for cardiomyocyte-specific gene deletion after birth. Non-invasive assessment of left ventricular (LV) chamber size and ejection performance used M-mode echocardiography performed on unsedated mice. Physiological measurements were performed on 6–8 week old mice. Invasive hemodynamic evaluation of LV contractile function and the response to atrial pacing or infused β_1 -adrenergic agonist, dobutamine, was performed using standard techniques as described. Analysis of isolated murine ventricular myocyte cell shortening and Ca^{2+} signaling was performed as described.^{25,26} All experimental procedures were approved by the Animal Studies Committee at Washington University School of Medicine.

Drosophila models and phenotypic analyses

The dMFN/MARF RNAi fly line used in this study was provided by Ming Guo.^{10,27} Rolf Bodmer (Sanford-Burnham Medical Research Institute, La Jolla, California) provided the *tincΔ4-Gal4* stock.²⁸ The GCaMP3.0 expressing *Drosophila* line was obtained from the Bloomington Stock Center (stock #32234). *In situ* analysis of working heart tube dimension and contraction by optical coherence tomography was as described.¹⁰ Ca^{2+} signal measurement from *in situ* heart tubes expressing GCaMP3.0 was performed on semi-intact 3-day-old adult flies. Flies were dissected and maintained in artificial hemolymph.²⁹ Cuts were made anterior to the abdomen, removing the head thorax and legs in one cut. The posterior abdominal segments were likewise removed. Lateral cuts along the abdominal cuticle were made on each side of the heart-tube. These cuts allowed for the removal of the ventral portion of the abdomen and revealed the beating heart-tube. To control for variability in heart rate between animals, specimens were kept on slides suspended over an ice bath chilled to 10°C. Phasic Ca^{2+} transients were captured over a 10 second period on a Nikon AZ100 UV fluorescent microscope at 100× magnification. Caffeine (10 mmol/L) was added to Nifedipine (300 μmol/L)-arrested heart tubes to stimulate full SR Ca^{2+} export. Change in fluorescence was measured over a 150×100 pixel area centered over the conical region of the heart tube. Images were acquired at ~150 frames per second using a Photometrics Evolve EMCCD camera. Image analysis was performed with Nikon NIS elements 3.0 Advanced software.

Ultrastructure studies by transmission electron microscopy (TEM)

A detailed description of these studies is given in the Online Supplement.

Immunoblot analyses

Mouse myocardial proteins were size-separated by 10% SDS-PAGE, transferred to PVDF membranes, and blocked with phosphate-buffered saline (PBS) and 0.1% Tween-20 (PBS-T) plus 5% nonfat dry milk before being incubated with primary antibodies: (Abcam mouse polyclonal anti-Mfn1 [1:1000 dilution], mouse monoclonal anti-Mfn2 [1:1000 dilution], Cell Signaling Rabbit polyclonal anti-SERCA [1:1000], Abcam mouse monoclonal anti-RYR [1:1000 dilution], Abcam mouse monoclonal anti-NCX1 [1:500], Santa Cruz goat polyclonal anti-PLN [1:1000], and Sigma mouse monoclonal anti-A-TUBULIN [1:5000 dilution]). Secondary antibody was goat anti-mouse immunoglobulin G (IgG), or goat anti-rabbit immunoglobulin G (IgG; 1:5000 dilution, Cell Signaling, Danvers, MA), or donkey anti-goat immunoglobulin G (IgG; 1:2000 dilution, Santa Cruz, CA) visualized using the ECL-Plus chemiluminescence reagent (GE Healthcare). Mitochondrial-associated membranes (MAMs) were obtained as described previously.³⁰

Measurement of $[Ca^{2+}]_m$ and $[Ca^{2+}]_c$ in isolated cardiomyocytes

LV cardiac myocytes were isolated by enzymatic digestion and recordings of $[Ca^{2+}]_m$ together with $[Ca^{2+}]_c$ were performed using a patch-clamp based approach as described previously.^{26,31} Briefly, myocytes were loaded with cell-permeable rhod-2 AM (for $[Ca^{2+}]_m$) and then patch-clamped and dialyzed with a pipette solution that contained a K^+ -glutamate based pipette solution (composition see Supplemental Information) containing cell-impermeable indo-1 salt to monitor $[Ca^{2+}]_c$. Myocytes were held at -70 mV in voltage-clamp mode and then depolarized to +10 mV for 100 ms at 0.5 Hz. After 60 s, isoproterenol (30 nmol/L) was added, and after 180 s, stimulation frequency was increased to 5 Hz (with depolarizing steps shortened to 50 ms). After 3 min, isoproterenol was washed out and stimulation frequency was set back to 0.5 Hz.

Fluorescence recordings in field-stimulated cardiomyocytes

Isolated cardiomyocytes were paced by electrical field stimulation using a customized IonOptix system as described previously.²⁶ The autofluorescences of NAD(P)H/NAD(P)⁺ and FADH₂/FAD were determined by alternately exciting cells at wavelengths (λ_{exc}) of 340 and 485 nm, and collecting emission at λ_{em} of 450 and 525 nm for NAD(P)H and FAD⁺, respectively. Calibration was performed with FCCP (5 μ mol/L) and cyanide (4 mmol/L).²⁶ To detect mitochondrial superoxide ($\cdot O_2^-$), myocytes were loaded with MitoSOX (3.3 μ mol/L) for 30 min at 37°C (λ_{exc} =380 nm, λ_{em} =580 nm). As a positive control, antimycin A (150 μ mol/L) was used. $[Ca^{2+}]_c$ was measured by incubating cells with indo-1 AM (5 μ mol/L) for 20 min at 25°C (λ_{exc} =340 nm, λ_{em} =405/485 nm). To monitor $\Delta\Psi_m$, myocytes were incubated with TMRM for 10 min at 25°C, and fluorescence intensity (λ_{exc} =540 nm, λ_{em} =605 nm) determined before and after application of FCCP (4 μ mol/L) and oligomycin (1.26 μ mol/L) to completely dissipate $\Delta\Psi_m$.

Mitochondrial swelling assay

Mitochondrial swelling assays were performed as reported previously.³²

L-type Ca²⁺ channel electrophysiological recordings

Experiments were performed as described previously³³ and as outlined in more detail in the Online Supplement.

Statistical analysis

Data are reported as means \pm SEM, respectively. P-values <0.05 were considered significant. For comparisons between 2 groups, unpaired t-test was performed unless indicated otherwise in the legend.

RESULTS

Cardiomyocyte SR Ca²⁺ release is increased in mitofusin-deficient *Drosophila* heart tubes

An essential role for mitofusin proteins in cardiac function was recently described in a *Drosophila* model wherein the single fruit fly mitofusin ortholog, MARF, was suppressed specifically in the heart tube.¹⁰ Loss of cardiomyocyte mitofusin/MARF produced mitochondrial fragmentation and dilated cardiomyopathy. Human and experimental cardiomyopathies induce characteristic alterations of cytosolic Ca²⁺ homeostasis.³⁴ As the consequences of mitofusin/MARF insufficiency on cardiomyocyte Ca²⁺ handling were unknown, we measured $[Ca^{2+}]_c$ in *Drosophila* heart tubes using an improved genetically-encoded Ca²⁺ indicator, GCaMP3.0.³⁵ Ca²⁺ measurements were performed in intact, spontaneously contracting heart tubes (Figure 1a; left). Cardiomyocyte-specific ryanodine receptor (RyR) deficiency in *Drosophila*, studied as a positive control for altered SR Ca²⁺ signaling, produced the expected decreases in Ca²⁺ transient amplitude in comparison to *tinc44-GAL4* controls (Figure 1a; right). By contrast, mitofusin/MARF-deficient fly heart tubes exhibited increased $[Ca^{2+}]_c$ transient amplitudes with normal time-constants for normalization (i.e. SR Ca²⁺ reuptake; Figure 1b), and larger amplitudes of caffeine-induced $[Ca^{2+}]_c$ transients (Figure 1c). To assure that concomitant cardiomyocyte-specific expression of the GCaMP3.0 Ca²⁺ probe had not altered the cardiomyopathic MARF RNAi cardiac phenotype previously described,¹⁰ we used optical coherence tomography to assess heart tube dimensions and contraction in the same flies used for the Ca²⁺ studies; the characteristic heart tube remodeling and contractile depression were unchanged (Figure 1d). Together, these findings indicate that cardiomyocyte-specific suppression of the fruit fly mitofusin ortholog, MARF, atypically alters SR Ca²⁺ handling.

Postnatal cardiac ablation of murine Mfn1 and Mfn2

Because *Drosophila* MARF is the single ortholog of both mammalian mitofusins, Mfn1 and Mfn2, the closest murine genetic counterpart to cardiomyocyte-specific MARF suppression is combined cardiomyocyte-specific ablation of *mfn1* and *mfn2*. We recently reported that cardiac Mfn1 and Mfn2 double knockout mice die at embryonic day 10.5, and observed that conditional combined Mfn1 and Mfn2 ablation in adult mouse hearts induced a rapidly progressive lethal dilated cardiomyopathy with mitochondrial fragmentation.¹¹ Within a week of tamoxifen-induced cardiac double *mfn* gene ablation, the $[Ca^{2+}]_c$ transients of Mfn1/Mfn2-deficient mouse cardiomyocytes suggested a trend toward increased amplitude.¹¹ Thus, our studies in both the *Drosophila* and murine cardiac mitofusin insufficiency models implicated these mitochondrial fusion proteins in cardiomyocyte Ca^{2+} signaling. Defining a specific mechanism whereby one or the other Mfn protein affected Ca^{2+} handling required selective ablation of *mfn1* or *mfn2* in the mouse heart to uncover specific effects of either mitofusin on cardiomyocyte Ca^{2+} handling without inducing mitochondrial fragmentation (because they are redundant for this function³⁻⁵). Accordingly, we crossed *mfn1* and *mfn2* floxed allele mice⁴ onto a *MYH6* directed nuclear-localized (“turbo”) Cre transgene²⁴ that induces gene recombination in cardiomyocytes beginning in the early postnatal period (Figure 2a–c) without confounding cardiotoxicity.^{18,36}

Mfn1 and Mfn2 cardiac-deficient mice were born at expected Mendelian ratios (Online Table I). Mfn1 and Mfn2 immunoreactivities were decreased by ~80% in the respective cardiac knockout mice, without compensatory upregulation of the non-targeted mitofusin (Figures 2a and 2b). LV dimension and ejection performance and the contractile responses at baseline and after β_1 -adrenergic stimulation with dobutamine were normal in 6 week old cardiac Mfn1- (Figures 2d and 2f) and Mfn2-KO mice (Figures 2e and 2g). Mfn2-mediated mitochondrial fusion has been linked to protection from apoptosis,³⁷ but there was no increase in TUNEL labeling or histological evidence of cardiomyocyte drop-out in Mfn2-deficient hearts (Online Figure I).

Mfn2-containing microdomains modulate SR Ca^{2+} handling

Mfn2 tethers mitochondria to the ER in mouse embryonic fibroblasts,¹² and physical tethering between ER and mitochondria is postulated to support microdomains through which Ca^{2+} transits between the organelles.¹⁴ Thus, disruption of these molecular tethers by ablation of Mfn2 may potentially also affect SR-mitochondrial Ca^{2+} signaling. To see if this paradigm applies to the mammalian heart, we measured cytosolic Ca^{2+} transients in ventricular cardiomyocytes from adult Mfn1- or Mfn2-deficient mice. Steady-state $[Ca^{2+}]_c$ transients of Mfn1-KO cardiomyocytes (Fura-2; field-stimulated at 1 Hz) exhibited normal peak amplitudes and decay kinetics (Figure 3a). By comparison, cardiomyocyte Mfn2-deficiency produced slightly increased peak amplitudes of $[Ca^{2+}]_c$ transients (Figure 3b). However, this increase was not associated with changes in the overall expression of Ca^{2+} transporting proteins in Mfn2-KO hearts (Figure 3c).

Increased $[Ca^{2+}]_c$ after electrical field stimulation is the consequence of Ca^{2+} influx through sarcolemmal L-type Ca^{2+} channels and Ca^{2+} release through SR RyRs.³⁸ In whole-cell voltage clamp recordings, L-type Ca^{2+} channel current ($I_{Ca,L}$) density was not different between Mfn2-KO and control myocytes (Figure 3d). An alternate explanation for the abnormally increased cardiomyocyte $[Ca^{2+}]_c$ amplitude in Mfn2-KO cardiomyocytes is increased SR Ca^{2+} load or decreased locally activated mitochondrial Ca^{2+} clearance. In fact, direct activation of RyRs by caffeine resulted in larger $[Ca^{2+}]_c$ increases in Mfn2-KO myocytes, while no difference was observed between Mfn1-KO and control myocytes (Figures 3e, 3f) The time constants (τ -values) for Ca^{2+} decay after caffeine, but also after steady-state Ca^{2+} transients were unchanged in Mfn1- and Mfn2-deficient myocytes

compared to their respective controls (Figures 3a, 3b and data not shown), indicating similar NCX and SR Ca²⁺ ATPase activities, respectively.

Cardiac Mfn2 deficiency impairs mitochondrial-SR tethering

These data raised the possibility that deletion of cardiomyocyte Mfn2 alters mitochondrial-SR Ca²⁺ cross-talk rather than primarily affecting cytosolic Ca²⁺ handling. To test this, we isolated cardiac mitochondria and examined the mitochondrial-associated membranes (MAMs, the shared ER/SR and mitochondrial membranes) for differences in SR protein content driven by Mfn ablation. Indeed, the content of SR-associated RyR2 protein in cardiac MAMs was strikingly depressed by Mfn2-ablation, compared to their respective controls (Figure 3g), despite unchanged overall cardiac RyR2 content (Figure 3c). Thus, the physical coupling to the mitochondria of the SR subdomains hosting RyR2 (terminal cisternae or junctional SR) became weaker upon Mfn2 ablation. Also in Mfn1 KO MAMs, RyR content appeared to be slightly diminished, however, the effect was clearly less pronounced than in Mfn2 KO hearts (Figure 3g), suggesting an unexplained, likely indirect, effect of Mfn1 ablation on SR-mitochondrial interactions. Alternatively, one could speculate that homotypic (Mfn2-Mfn2) SR-mitochondrial tether formation cannot compensate 100% for the loss of the heterotypic (SR Mfn2 – mitochondrial Mfn1) tethers in Mfn1 KO hearts.

To further investigate mitochondrial morphology and in particular, SR-mitochondrial interaction, we analyzed transmission electron micrographs (TEM) of Mfn1- and Mfn2-KO and their respective control hearts (Figure 4). In agreement with the data of Papanicolaou et al.,¹⁸ the mitochondrial area was increased in Mfn2 KO hearts (Figure 4a and 4c, top) without an increase in the mitochondrial area density (relative to sarcoplasmic area; data not shown). Likewise, the major axis of a fitted ellipse was longer in the Mfn2 KO mitochondria (1.35±0.025 μm vs 1.09±0.01 μm; n=978 and 1317 in Mfn2 KO and control hearts, respectively; p<0.05). The transversal side length of mitochondria in close association with junctional SR (jSR) was unchanged with Mfn2 ablation (Figure 4c, bottom left), but the transversal side segment forming an interface with jSR was reduced by ~30% in Mfn2 KO vs. control hearts (Figure 4c, bottom right). Furthermore, there was a trend towards an increase in the mean distance between jSR and the outer mitochondrial membrane in Mfn2 KO versus control hearts (by ~17%; p=0.07; data not shown). In contrast, none of these parameters were altered in Mfn1 KO hearts compared to their respective controls (Figure 4b). Taken together, loss of Mfn2, but not Mfn1, substantially diminishes the physical interaction between SR and mitochondria in cardiac myocytes.

Ablation of cardiac Mfn2, but not Mfn1, disrupts the mitochondrial bioenergetic response

To test whether the alterations of SR-mitochondrial interaction affect mitochondrial Ca²⁺ uptake under physiological conditions, we applied a patch-clamp based approach that we previously established in guinea-pig cardiac myocytes.^{26,31,39} Intact murine cardiac myocytes were loaded with the cell-permeable Ca²⁺-indicator rhod-2 AM, which locates primarily to mitochondria. To eliminate contaminating signals from cytosol-located rhod-2 traces, myocytes were whole-cell patch clamped and dialyzed with a pipette solution that did not contain rhod-2, but (membrane-impermeable) indo-1 salt. With this technique, we monitored [Ca²⁺]_m (by rhod-2) together with [Ca²⁺]_c (by indo-1) in “working” cardiac myocytes that were voltage-clamped and depolarized to +10 mV at 0.5 Hz, inducing steady-state Ca²⁺ transients. To impose a near physiological workload, isoproterenol was applied and the rate of depolarization was increased to 5 Hz for 3 min (Figure 5b, 5d). In agreement with our previous results,^{31,39} rapid mitochondrial Ca²⁺ transients were observed during cytosolic Ca²⁺ transients, with diastolic accumulation of [Ca²⁺]_m during β-adrenergic stimulation and an increase in pacing rate (Figures 5a–d). To rule out that beat-to-beat [Ca²⁺]_m transients reported by rhod-2 derived from cytosolic traces of the dye, we

performed control experiments with an inhibitor of the MCU (1 $\mu\text{mol/L}$ of Ru360 in the pipette solution; Online Figure II). Ru360 reduced the amplitude of $[\text{Ca}^{2+}]_m$, but not $[\text{Ca}^{2+}]_c$ transients and blunted the diastolic accumulation of $[\text{Ca}^{2+}]_m$, confirming specific localization of rhod-2 to mitochondria (Online Figure II and refs^{31, 39}).

While in Mfn1-deficient myocytes, mitochondrial Ca^{2+} uptake was unchanged compared to control myocytes (Figures 5a, 5b), the dynamic relationship between $[\text{Ca}^{2+}]_m$ and $[\text{Ca}^{2+}]_c$ was shifted toward lower efficiency of mitochondrial Ca^{2+} uptake in Mfn2-deficient myocytes (Figure 5c). At 0.5 Hz, mitochondrial Ca^{2+} accumulation in response to β -adrenergic stimulation was completely blunted in Mfn2-KO myocytes compared to controls (Figure 5d and inset). At 5 Hz and maintained presence of isoproterenol, mitochondrial Ca^{2+} accumulation remained decreased in Mfn2-KO myocytes compared to controls, however, equilibrated in the course of this stimulation to similar levels (Figure 5d).

To further elucidate whether the differences in mitochondrial Ca^{2+} accumulation in Mfn2-KO and WT myocytes were related to differences in mitochondrial Ca^{2+} uptake and/or decay kinetics, we determined the time-to-peak (TTP) and time to 50% decay (RT_{50}) of cytosolic and mitochondrial Ca^{2+} transients, respectively. In agreement with our previous results,^{31,39} the TTP of $[\text{Ca}^{2+}]_m$ was faster than of $[\text{Ca}^{2+}]_c$ in WT myocytes, supporting the concept that mitochondria may sense Ca^{2+} from a microdomain that is closer to RyRs than the bulk cytosol (Online Figure IIIa). While TTP of $[\text{Ca}^{2+}]_c$ was unchanged between Mfn2-KO and WT myocytes, TTP of $[\text{Ca}^{2+}]_m$ was slightly, but consistently delayed in Mfn2-KO myocytes compared to control myocytes (Online Figures IIIb and IIIc). In contrast, RT_{50} values of $[\text{Ca}^{2+}]_c$ and $[\text{Ca}^{2+}]_m$ were unchanged in both genotypes (Online Figures IIIb and IIIc), indicating that differential mitochondrial Ca^{2+} accumulation is related to defects in mitochondrial Ca^{2+} uptake rather than export.

In the mitochondrial matrix, Krebs cycle dehydrogenases are activated by Ca^{2+} , accelerating the regeneration of NAD(P)H and FADH_2 from NAD(P)⁺ and FAD.^{6,7} Thus, the redox states of NAD(P)H/NAD(P)⁺ and FADH_2/FAD and in particular, the ratio of NAD(P)H/FAD, serve as sensitive and ratiometric read-outs of Ca^{2+} -induced Krebs cycle activation.^{26,40} Furthermore, these redox states can be obtained in intact (unpatched) myocytes, avoiding cell dialysis with a pipette solution and thus, conserving the physiological intracellular milieu. Myocytes were field-stimulated with a similar protocol as for $[\text{Ca}^{2+}]_c/[\text{Ca}^{2+}]_m$ recordings (Online Figure IV). In agreement with unchanged mitochondrial Ca^{2+} uptake (Figure 5a, 5b), the redox states of NAD(P)H/NAD(P)⁺ and FADH_2/FAD remained constant over the course of the protocol in Mfn1-KO myocytes (Figure 5e). In contrast, NAD(P)H and FADH_2 were oxidized in Mfn2-KO compared to control myocytes at 0.5 Hz in the presence of isoproterenol, reflecting a mismatch between NADH and FADH_2 oxidation by the respiratory chain (through ADP-induced acceleration of respiration⁷) and Krebs cycle-induced re-reduction. Similar increases in sarcomere shortening and cytosolic Ca^{2+} transient amplitudes indicated similar workloads in both groups (Online Figure IV), making differences in Ca^{2+} -induced Krebs cycle activation the most likely explanation for net NAD(P)H and FAD oxidation. As reduced NADPH is required for elimination of ROS from the matrix,³¹ mitochondrial $\cdot\text{O}_2^-$ production was temporarily increased by isoproterenol challenge of Mfn2-KO cardiomyocytes (Figure 6a).

The observed bioenergetic and redox mismatches in Mfn2-deficient cardiomyocytes were not related to an intrinsic defect in mitochondrial Ca^{2+} uptake because both the mitochondrial membrane potential ($\Delta\Psi_m$) as the driving force for mitochondrial Ca^{2+} uptake (Figure 6b) and Ca^{2+} sensitivity of mitochondrial swelling (Figure 6c) were similar. These results suggest that Mfn2 plays a role in the regulation of SR-mitochondrial calcium crosstalk, but not intrinsic mitochondrial sensitivity to Ca^{2+} . Furthermore, similar $\Delta\Psi_m$

values (Figure 6b) and similar cardiomyocyte performance at elevated work (Online Figure IV) suggest that Mfn2-deficiency had no direct impact on respiratory chain function or ATP production.

DISCUSSION

In the studies of genetically manipulated *Drosophila* heart tubes and mouse hearts detailed here, we provide evidence that Mfn2 bridges cardiomyocyte SR and mitochondria, thus facilitating inter-organelle Ca^{2+} crosstalk that regulates the immediate bioenergetic response to increased cardiac work. This function of Mfn2 is not shared by Mfn1, and appears independent of effects on mitochondrial fusion.^{4,5,11}

The concentration and contextual release of Ca^{2+} , a ubiquitous signaling molecule, are linked to a variety of essential physiological as well as many pathological cellular processes. Intracellular Ca^{2+} is heavily sequestered within storage organelles, largely SR/ER, thus maintaining relatively low levels of $[\text{Ca}^{2+}]_c$. In cardiac myocytes, $[\text{Ca}^{2+}]_c$ oscillates from a baseline (diastolic) concentration of ~ 100 nM to a peak level of ~ 1 μM with each cardiac systole. A small fraction of this Ca^{2+} enters through sarcolemmal L-type Ca^{2+} channels, but the majority is released from SR via RyRs, and taken up again via SR Ca^{2+} ATPase.^{7,38}

Mitochondria are essential to cardiac SR Ca^{2+} cycling as the source of ATP that fuels various ion pumps and myosin ATPase. Accordingly, SR and mitochondria are organized throughout cardiac myocytes in an intricate and intimate physical association. Spatial co-localization of mitochondria with SR facilitates compartmentalization and privileged trans-organelle transport of ATP, and potentially also for Ca^{2+} . In mitochondria, Ca^{2+} plays a key role in matching energy supply and demand by stimulating rate-limiting enzymes of the Krebs cycle, the main producer of NADH.^{6,7} Since regeneration of antioxidative NADPH is coupled to the Krebs cycle, mitochondrial Ca^{2+} uptake also plays an important role in preventing excess formation of toxic ROS.³¹ However, the low Ca^{2+} affinity of the primary mitochondrial Ca^{2+} uptake mechanism (i.e., the MCU; $\text{EC}_{50} \sim 10$ mM⁴¹) limits the ability of mitochondria to import Ca^{2+} from the cytosol, where Ca^{2+} levels are normally much lower.¹⁴ To resolve this apparent paradox, Rizzuto and Pozzan inferred the existence of Ca^{2+} signaling “hot-spots”, or microdomains, between ER and mitochondria.^{42,43} Indirect evidence has previously pointed to a role for localized SR-mitochondrial Ca^{2+} signaling in cardiac myocytes⁴⁴⁻⁴⁶ and (although the molecular mediator was unknown) SR-mitochondrial bridging has been observed in heart and striated muscle.^{47,48} Csordas, Hajnoczky, and colleagues defined structural and functional mitochondrial-ER connections,^{13,49} and de Brito and Scorrano established a molecular mechanism for physical tethering of mitochondria to ER by Mfn2 in embryonic fibroblasts.¹²

Our results demonstrate that the concept proposed by de Brito and Scorrano of Mfn2 as a molecular tether between ER and mitochondria¹² is applicable to the SR in the distinct sub-cellular structure and organ physiology of the heart, in which the SR is the main Ca^{2+} store. The heart is the most mitochondria-rich organ and requires high and quickly modifiable rates of ATP generation to maintain organ pumping function under different work loads. Cardiac EC coupling is dependent upon constant cyclic SR Ca^{2+} release and re-uptake.³⁸ Disturbances in either mitochondrial metabolism or SR Ca^{2+} cycling induce cardiac dysfunction and can cause heart disease.^{50,51} For these reasons, we postulated that the unique sensitivity of the heart to reticular and mitochondrial dysfunction would make it an ideal experimental platform in which the molecular determinants of mitochondrial-SR crosstalk could be functionally interrogated. Our findings reveal that SR-mitochondrial tethering by Mfn2 is essential for mitochondrial sensing of stress-induced SR Ca^{2+} release, linking mitochondrial ATP production to SR Ca^{2+} cycling in a rapid-response system that

prevents bioenergetic lag when cardiac work is acutely increased. However, we cannot exclude the possibility that also other proteins – such as PACS-2 or IP₃-receptors interacting with VDAC in the ER-mitochondrial interaction of other cell types^{19,20} – may contribute to SR-mitochondrial crosstalk in cardiac myocytes.

While our findings confirm and expand upon those of de Brito and Scorrano,¹² they contrast with those of Papanicolaou et al¹⁸ who recently reported that cardiac-specific ablation of Mfn2 in mice does not alter the close associations between SR and mitochondria (based on distance measurements) or affect cardiomyocyte Ca²⁺ signaling, and that loss of Mfn2 protected against ischemia-induced opening of the mitochondrial permeability transition pore.¹⁸ There are important differences between our studies and those of Papanicolaou and colleagues. First, the Cre line used in the previous study is well known to express Cre at sufficiently high levels in the mouse embryo and adult that it induces cardiotoxicity in older mice.²² The nuclear-directed Cre line employed in our studies induces recombination only after birth (vide supra) and has not been reported to induce any toxicity.²² Indeed, since the same Cre excision strategy was used in our parallel experiments for both Mfn1 and Mfn2, direct Cre effects have not contributed to our findings.

Second, for the critical issue of whether ablation of Mfn2 from cardiac myocytes alters the close associations between SR and mitochondria, i.e. whether Mfn2 actually tethers the two organelles as described by de Brito and Scorrano, differences in the morphometric analysis may explain Papanicolaou's negative findings. Their analysis was restricted to measurements of the distance between the center of T-tubules and mitochondria, which was in the range of 150 nm and not different between Mfn2-KO and control animals.¹⁸ In contrast, we analyzed the distance between the junctional SR and mitochondria, which is in the range of only 15 nm and a more direct parameter for SR-mitochondrial tethering than the distance from the T-tubule center to mitochondria. In these measurements we observed a trend towards a widening of the gap between SR and mitochondria in Mfn2-KO compared to control mice (p=0.07). Moreover, another important parameter for the functional interaction between SR and mitochondria is the actual contact length of mitochondria with the junctional SR, which was decreased by ~30% in Mfn2-KO, but not Mfn1-KO hearts in our study but was not analyzed in the study of Papanicolaou et al.¹⁸ As the SR-mitochondrial physical coupling is predicted to be established by more than one tether species,⁵² eliminating only one of these tethers (Mfn2) may decrease interface formation with or without a change in the gap distance of the remaining associations. These ultrastructural differences were corroborated by the substantially decreased content of SR-specific RyRs in mitochondria-associated membranes (MAMs) isolated from Mfn2-KO (but not Mfn1-KO) hearts, demonstrating a mechanically more vulnerable coupling between SR and mitochondria.

The kinetics of mitochondrial Ca²⁺ uptake are still subject to debate,^{7,15–17} which is primarily related to the low affinity of the MCU for Ca²⁺ and differential results yielded by the use of different techniques. While some observers have described beat-to-beat cardiomyocyte mitochondrial Ca²⁺ transients, others have observed only slow Ca²⁺ accumulation during increases of the amplitudes and/or rate of cytosolic Ca²⁺ transients.^{7,15–17} The existence of RyR-derived high Ca²⁺ microdomains facilitating Ca²⁺ delivery to mitochondria was inferred from data in permeabilized H9c2 myotubes⁴⁴ and cardiomyocytes.⁴⁵ We have also previously used computational modeling and electrophysiological studies to support the existence of Ca²⁺ microdomains between closely associated mitochondria and SR, within which “hot spots” of Ca²⁺ can accumulate at sufficiently high concentrations (because of limited diffusion) to be imported by the low affinity MCU.^{26,31,39} Here, we demonstrate that Mfn2 is a critical structural component to these microdomains and to mitochondrial uptake of Ca²⁺ release from juxtaposed SR. The

weakened associations of jSR and mitochondria in Mfn2-ablated cardiomyocytes lead to increased pacing- as well as caffeine-triggered $[Ca^{2+}]_c$ signal amplitudes without changes in the expression levels of SR Ca^{2+} handling proteins, or in the activity of high-affinity Ca^{2+} extrusion mechanisms (SERCA, NCX). Thus, these increased $[Ca^{2+}]_c$ signals were not likely to be due to enhanced SR Ca^{2+} accumulation or decreased sarcolemmal Ca^{2+} extrusion but rather to the decreased local mitochondrial Ca^{2+} clearance.

The primary physiological role of mitochondrial Ca^{2+} uptake is the stimulation of rate-limiting enzymes of the Krebs cycle to adapt energy supply and demand.^{6,7} In fact, the redox states of NAD(P)H/NAD(P)⁺ and FADH₂/FAD⁺, and the ratio of NAD(P)H/FAD⁺ (an index of the balance between Krebs cycle-induced reduction versus oxidation through the respiratory chain) were more oxidized during β -adrenergic stimulation in Mfn2-KO than in control cardiomyocytes. Furthermore, we recently discovered that mitochondrial Ca^{2+} uptake during β -adrenergic stimulation prevents mitochondrial ROS formation by buffering the NADPH-dependent antioxidative capacity.³¹ Indeed, mitochondrial O₂- increased slightly within the first minute of isoproterenol, which may be related to oxidation of NADPH secondary to a mismatch of ADP-induced oxidation and Ca^{2+} -induced reduction of NAD(P)H.³¹ Suppression of *Drosophila* mitofusin ortholog, MARF, induced dilated cardiomyopathy and cardiomyocyte mitochondrial fragmentation; the former was improved by cardiac expression of superoxide dismutase whereas the latter was not.¹⁰ This observation and the differences between single Mfn1 and Mfn2 cardiac knockout mice described here and double Mfn1/Mfn2 cardiac knockout mice recently reported further emphasize the different roles of mitofusins as mediators of mitochondrial fusion, and as modulators of SR-mitochondria Ca^{2+} transport/bioenergetics/ROS production. Our data suggest that the defects in the spatial organization of mitochondria and SR which depress mitochondrial Ca^{2+} uptake may also contribute to myocardial oxidative stress.

Supplementary Material

Refer to Web version on PubMed Central for supplementary material.

Acknowledgments

SOURCES OF FUNDING

Supported by NIH/NHLBI HL59888 (to GWD) and HL034161 (to JMN). C. M. is supported by Deutsche Forschungsgemeinschaft (Emmy Noether Programm, KFO 196 and SFB 894). MK is supported by HOMFOR *excellent*.

Non-standard Abbreviations

$[Ca^{2+}]_c$	cytosolic Ca^{2+} concentration
$[Ca^{2+}]_m$	mitochondrial Ca^{2+} concentration
$\Delta\Psi_m$	mitochondrial membrane potential
EC	excitation-contraction
ER	endoplasmic reticulum
SR	sarcoplasmic reticulum
IP ₃	inositol-trisphosphate
jSR	junctional SR
LV	left ventricular

MARF	mitochondrial assembly regulatory factor
MCU	mitochondrial Ca ²⁺ uniporter
Mfn	mitofusin
ROS	reactive oxygen species

REFERENCES

1. Campello S, Scorrano L. Mitochondrial shape changes: orchestrating cell pathophysiology. *EMBO Rep.* 2010; 11:678–684. [PubMed: 20725092]
2. Chen H, Chan DC. Physiological functions of mitochondrial fusion. *Ann. N. Y. Acad. Sci.* 2010; 1201:21–25. [PubMed: 20649534]
3. Chen H, Chomyn A, Chan DC. Disruption of fusion results in mitochondrial heterogeneity and dysfunction. *J. Biol. Chem.* 2005; 280:26185–26192. [PubMed: 15899901]
4. Chen H, McCaffery JM, Chan DC. Mitochondrial fusion protects against neurodegeneration in the cerebellum. *Cell.* 2007; 130:548–562. [PubMed: 17693261]
5. Chen H, Vermulst M, Wang YE, Chomyn A, Prolla TA, McCaffery JM, Chan DC. Mitochondrial fusion is required for mtDNA stability in skeletal muscle and tolerance of mtDNA mutations. *Cell.* 2010; 141:280–289. [PubMed: 20403324]
6. Balaban RS. Domestication of the cardiac mitochondrion for energy conversion. *J Mol Cell Cardiol.* 2009; 46:832–841. [PubMed: 19265699]
7. Maack C, O'Rourke B. Excitation-contraction coupling and mitochondrial energetics. *Basic Res Cardiol.* 2007; 102:369–392. [PubMed: 17657400]
8. Archer SL. The mitochondrion as a Swiss army knife: implications for cardiovascular disease. *J. Mol. Med.* 2010; 88:963–965. [PubMed: 20711556]
9. Kane LA, Youle RJ. Mitochondrial fission and fusion and their roles in the heart. *J. Mol. Med.* 2010; 88:971–979. [PubMed: 20835916]
10. Dorn GW 2nd, Clark CF, Eschenbacher WH, Kang MY, Engelhard JT, Warner SJ, Matkovich SJ, Jowdy CC. MARF and Opa1 control mitochondrial and cardiac function in *Drosophila*. *Circ. Res.* 2011; 108:12–17. [PubMed: 21148429]
11. Chen Y, Liu Y, Dorn GW. Mitochondrial Fusion is Essential for Organelle Function and Cardiac Homeostasis. *Circ. Res* (2nd.). 2011; 109:1327–1331. [PubMed: 22052916]
12. de Brito OM, Scorrano L. Mitofusin 2 tethers endoplasmic reticulum to mitochondria. *Nature.* 2008; 456:605–610. [PubMed: 19052620]
13. Csordas G, Renken C, Varnai P, Walter L, Weaver D, Buttle KF, Balla T, Mannella CA, Hajnoczky G. Structural and functional features and significance of the physical linkage between ER and mitochondria. *J. Cell. Biol.* 2006; 174:915–921. [PubMed: 16982799]
14. Rizzuto R, Pozzan T. Microdomains of intracellular Ca²⁺: Molecular determinants and functional consequences. *Physiol. Rev.* 2006; 86:369–408. [PubMed: 16371601]
15. O'Rourke B, Blatter LA. Mitochondrial Ca²⁺ uptake: tortoise or hare? *J Mol Cell Cardiol.* 2009; 46:767–774. [PubMed: 19162034]
16. Dedkova EN, Blatter LA. Mitochondrial Ca²⁺ and the heart. *Cell Calcium.* 2008; 44:77–91. [PubMed: 18178248]
17. Chikando AC, Kettlewell S, Williams GS, Smith G, Lederer WJ. Ca²⁺ dynamics in the mitochondria - state of the art. *J Mol Cell Cardiol.* 2011; 51:627–631. [PubMed: 21864537]
18. Papanicolaou KN, Khairallah RJ, Ngoh GA, Chikando A, Luptak I, O'Shea KM, Riley DD, Lugas JJ, Colucci WS, Lederer WJ, Stanley WC, Walsh K. Mitofusin-2 maintains mitochondrial structure and contributes to stress-induced permeability transition in cardiac myocytes. *Mol. Cell. Biol.* 2011; 31:1309–1328. [PubMed: 21245373]
19. Simmen T, Aslan JE, Blagoveshchenskaya AD, Thomas L, Wan L, Xiang Y, Feliciangeli SF, Hung CH, Crump CM, Thomas G. PACS-2 controls endoplasmic reticulum-mitochondria communication and Bid-mediated apoptosis. *EMBO J.* 2005; 24:717–729. [PubMed: 15692567]

20. Szabadkai G, Bianchi K, Varnai P, De Stefani D, Wieckowski MR, Cavagna D, Nagy AI, Balla T, Rizzuto R. Chaperone-mediated coupling of endoplasmic reticulum and mitochondrial Ca²⁺ channels. *J. Cell. Biol.* 2006; 175:901–911. [PubMed: 17178908]
21. Wei AC, Aon MA, O'Rourke B, Winslow RL, Cortassa S. Mitochondrial energetics, pH regulation, and ion dynamics: a computational-experimental approach. *Biophys. J.* 2011; 100:2894–2903. [PubMed: 21689522]
22. Molkenin JD, Robbins J. With great power comes great responsibility: using mouse genetics to study cardiac hypertrophy and failure. *J. Mol. Cell. Cardiol.* 2009; 46:130–136. [PubMed: 18845155]
23. Chen H, Detmer SA, Ewald AJ, Griffin EE, Fraser SE, Chan DC. Mitofusins Mfn1 and Mfn2 coordinately regulate mitochondrial fusion and are essential for embryonic development. *J. Cell. Biol.* 2003; 160:189–200. [PubMed: 12527753]
24. van Berlo JH, Elrod JW, van den Hoogenhof MM, York AJ, Aronow BJ, Duncan SA, Molkenin JD. The transcription factor GATA-6 regulates pathological cardiac hypertrophy. *Circ. Res.* 2010; 107:1032–1040. [PubMed: 20705924]
25. Diwan A, Matkovich SJ, Yuan Q, Zhao W, Yatani A, Brown JH, Molkenin JD, Kranias EG, Dorn GWn. Endoplasmic reticulum-mitochondria crosstalk in NIX-mediated murine cell death. *J. Clin. Invest.* 2009; 119:203–212. [PubMed: 19065046]
26. Kohlhaas M, Maack C. Adverse bioenergetic consequences of Na⁺-Ca²⁺ exchanger-mediated Ca²⁺ influx in cardiac myocytes. *Circulation.* 2010; 122:2273–2280. [PubMed: 21098439]
27. Deng H, Dodson MW, Huang H, Guo M. The Parkinson's disease genes pink1 and parkin promote mitochondrial fission and/or inhibit fusion in *Drosophila*. *Proc Natl Acad Sci U S A.* 2008; 105:14503–14508. [PubMed: 18799731]
28. Lo PC, Frasch M. A role for the COUP-TF-related gene seven-up in the diversification of cardioblast identities in the dorsal vessel of *Drosophila*. *Mech. Dev.* 2001; 104:49–60. [PubMed: 11404079]
29. Broadie KS, Bate M. Development of the embryonic neuromuscular synapse of *Drosophila melanogaster*. *J. Neurosci.* 1993; 13:144–166. [PubMed: 8093713]
30. Chen Y, Lewis W, Diwan A, Cheng EH, Matkovich SJ, Dorn GW 2nd. Dual autonomous mitochondrial cell death pathways are activated by Nix/BNip3L and induce cardiomyopathy. *Proc Natl Acad Sci U S A.* 2010; 107:9035–9042. [PubMed: 20418503]
31. Kohlhaas M, Liu T, Knopp A, Zeller T, Ong MF, Böhm M, O'Rourke B, Maack C. Elevated cytosolic Na⁺ increases mitochondrial formation of reactive oxygen species in failing cardiac myocytes. *Circulation.* 2010; 121:1606–1613. [PubMed: 20351235]
32. Baines CP, Kaiser RA, Purcell NH, Blair NS, Osinska H, Hambleton MA, Brunskill EW, Sayen MR, Gottlieb RA, Dorn GW, Robbins J, Molkenin JD. Loss of cyclophilin D reveals a critical role for mitochondrial permeability transition in cell death. *Nature.* 2005; 434:658–662. [PubMed: 15800627]
33. Yang KC, Foeger NC, Marionneau C, Jay PY, McMullen JR, Nerbonne JM. Homeostatic regulation of electrical excitability in physiological cardiac hypertrophy. *J Physiol.* 2010; 588:5015–5032. [PubMed: 20974681]
34. Bers DM. Altered cardiac myocyte Ca regulation in heart failure. *Physiology (Bethesda).* 2006; 21:380–387. [PubMed: 17119150]
35. Seelig JD, Chiappe ME, Lott GK, Dutta A, Osborne JE, Reiser MB, Jayaraman V. Two-photon calcium imaging from head-fixed *Drosophila* during optomotor walking behavior. *Nat. Methods.* 2010; 7:535–540. [PubMed: 20526346]
36. Gaussin V, Van de Putte T, Mishina Y, Hanks MC, Zwijsen A, Huylebroeck D, Behringer RR, Schneider MD. Endocardial cushion and myocardial defects after cardiac myocyte-specific conditional deletion of the bone morphogenetic protein receptor ALK3. *Proc. Natl. Acad. Sci. USA.* 2002; 99:2878–2883. [PubMed: 11854453]
37. Neuspiel M, Zunino R, Gangaraju S, Rippstein P, McBride H. Activated mitofusin 2 signals mitochondrial fusion, interferes with Bax activation, and reduces susceptibility to radical induced depolarization. *J. Biol. Chem.* 2005; 280:25060–25070. [PubMed: 15878861]

38. Bers DM. Calcium cycling and signaling in cardiac myocytes. *Annu. Rev. Physiol.* 2008; 70:23–49. [PubMed: 17988210]
39. Maack C, Cortassa S, Aon MA, Ganesan AN, Liu T, O'Rourke B. Elevated cytosolic Na⁺ decreases mitochondrial Ca²⁺ uptake during excitation-contraction coupling and impairs energetic adaptation in cardiac myocytes. *Circ. Res.* 2006; 99:172–182. [PubMed: 16778127]
40. Hajnoczky G, Robb-Gaspers LD, Seitz MB, Thomas AP. Decoding of cytosolic calcium oscillations in the mitochondria. *Cell.* 1995; 82:415–424. [PubMed: 7634331]
41. Kirichok Y, Krapivinsky G, Clapham DE. The mitochondrial calcium uniporter is a highly selective ion channel. *Nature.* 2004; 427:360–364. [PubMed: 14737170]
42. Rizzuto R, Brini M, Murgia M, Pozzan T. Microdomains with high Ca²⁺ close to IP₃-sensitive channels that are sensed by neighboring mitochondria. *Science.* 1993; 262:744–747. [PubMed: 8235595]
43. Rizzuto R, Pinton P, Carrington W, Fay FS, Fogarty KE, Lifshitz LM, Tuft RA, Pozzan T. Close contacts with the endoplasmic reticulum as determinants of mitochondrial Ca²⁺ responses. *Science.* 1998; 280:1763–1766. [PubMed: 9624056]
44. Szalai G, Csordas G, Hantash BM, Thomas AP, Hajnoczky G. Calcium signal transmission between ryanodine receptors and mitochondria. *J. Biol. Chem.* 2000; 275:15305–15313. [PubMed: 10809765]
45. Sharma VK, Ramesh V, Franzini-Armstrong C, Sheu SS. Transport of Ca²⁺ from sarcoplasmic reticulum to mitochondria in rat ventricular myocytes. *J Bioenerg Biomembr.* 2000; 32:97–104. [PubMed: 11768767]
46. Garcia-Perez C, Hajnoczky G, Csordas G. Physical coupling supports the local Ca²⁺ transfer between sarcoplasmic reticulum subdomains and the mitochondria in heart muscle. *J. Biol. Chem.* 2008; 283:32771–32780. [PubMed: 18790739]
47. Hayashi T, Martone ME, Yu Z, Thor A, Doi M, Holst MJ, Ellisman MH, Hoshijima M. Three-dimensional electron microscopy reveals new details of membrane systems for Ca²⁺ signaling in the heart. *J. Cell Sci.* 2009; 122:1005–1013. [PubMed: 19295127]
48. Boncompagni S, Rossi AE, Micaroni M, Beznoussenko GV, Polishchuk RS, Dirksen RT, Protasi F. Mitochondria are linked to calcium stores in striated muscle by developmentally regulated tethering structures. *Mol. Biol. Cell.* 2009; 20:1058–1067. [PubMed: 19037102]
49. Csordas G, Thomas AP, Hajnoczky G. Quasi-synaptic calcium signal transmission between endoplasmic reticulum and mitochondria. *EMBO J.* 1999; 18:96–108. [PubMed: 9878054]
50. Huss JM, Kelly DP. Mitochondrial energy metabolism in heart failure: a question of balance. *J. Clin. Invest.* 2005; 115:547–555. [PubMed: 15765136]
51. Wehrens XH, Marks AR. Novel therapeutic approaches for heart failure by normalizing calcium cycling. *Nat. Rev. Drug Discovery.* 2004; 3:565–573.
52. Dorn GW 2nd, Scorrano L. Two close, too close: sarcoplasmic reticulum-mitochondrial crosstalk and cardiomyocyte fate. *Circ Res.* 2011; 107:689–699. [PubMed: 20847324]

Novelty and Significance

What is Known?

- Mitofusin 2 tethers endoplasmic reticulum to mitochondria in embryonic fibroblasts.
- Mitochondrial Ca^{2+} uptake is important for matching energy supply and demand and control mitochondrial emission of reactive oxygen species.
- In cardiac myocytes, mechanisms that tether sarcoplasmic reticulum (SR) to the mitochondria are unclear and the role of calcium crosstalk remains unknown.

What New Information Does This Article Contribute?

- In adult cardiac myocytes, mitofusin 2, but not mitofusin 1 tethers the SR. Tethering creates Ca^{2+} microdomains between the organelles that affects mitochondrial Ca^{2+} handling.
- SR-mitochondrial Ca^{2+} crosstalk via microdomains directs mitochondrial metabolism to increased contractile demand, avoiding bioenergetic mismatch and oxidative stress.

The heart consumes large amounts of energy that needs to be produced by mitochondria. For efficient energy regeneration, mitochondria take up Ca^{2+} that stimulates key enzymes of the Krebs cycle to increase the production of substrates of the electron transport chain. Since the mitochondrial Ca^{2+} uniporter has a relatively low affinity for Ca^{2+} , the kinetics of mitochondrial Ca^{2+} uptake are currently unclear. Here, we identify mitofusin 2 as a protein that tethers mitochondria to the SR, providing a close spatial interaction between both organelles that accounts for efficient mitochondrial Ca^{2+} uptake during changes of cardiac workload. At the same time, mitochondrial Ca^{2+} uptake shapes cytosolic Ca^{2+} signals. This function of mitofusin 2 is not related to its role in mitochondrial fusion and is not shared by its closely related homologue, mitofusin 1. Disruption of SR-mitochondrial Ca^{2+} crosstalk hampers energy supply-and-demand and may produce oxidative stress. These results demonstrate an essential physiological function of SR-mitochondrial tethering in controlling SR-to-mitochondria calcium delivery and matching mitochondrial bioenergetics to acute cardiac demand.

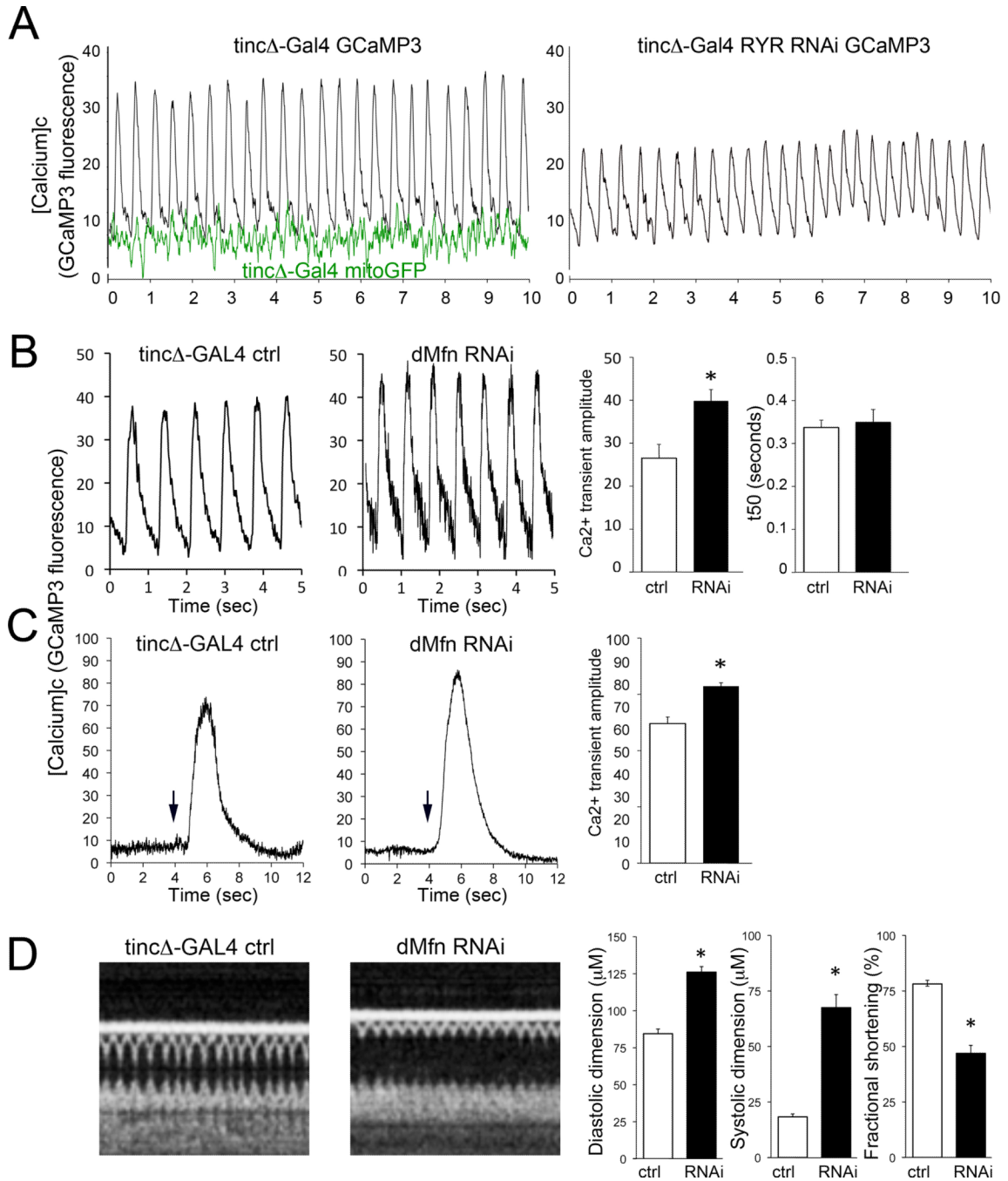


Figure 1. SR Ca²⁺ handling is altered by dMfn/MARF suppression in *Drosophila* heart tubes
A. (*left*) Representative Ca²⁺ transients monitored by fluorescence of GCaMP3.0 expressed specifically in cardiac myocytes of spontaneously contracting *Drosophila* heart tubes *in situ*. Black tracings are tinc Δ -Gal4-driven GCaMP3 (controls); green tracings are tinc Δ -Gal4 driven mitoGFP (which is Ca²⁺-insensitive), demonstrating minimal effects of heart tube contraction on fluorescence signals. (*right*) Representative tracing of RyR-deficient *Drosophila* heart tube, showing decreased amplitude and delayed normalization of Ca²⁺ transient, which is typical of heart failure. **B.** Ca²⁺ transients of control (ctrl; tinc Δ -Gal4) and mitofusin/MARF deficient (dMfn RNAi) expressing RNAi for dMfn. Representative

tracings are shown to the left and group data from n=11 individual flies are to the right. **C.** SR Ca^{2+} content measured as caffeine-stimulated cardiomyocyte Ca^{2+} release in heart tubes of dMfn deficient (RNAi) and ctrl flies. Representative tracings are shown to the left with arrows marking the time of caffeine (10 mM) addition; group data from n=5 or 6 individual flies are to the right. *p<0.05 vs ctrl. **D.** Heart tube dimensions and contractile function in control and dMfn RNAi *Drosophila*, assessed by optical coherence tomography (OCT). Representative b-mode OCT scans are shown on the left, with group data from the same set of flies that underwent Ca^{2+} measurements shown to the right. *p<0.05 vs ctrl.

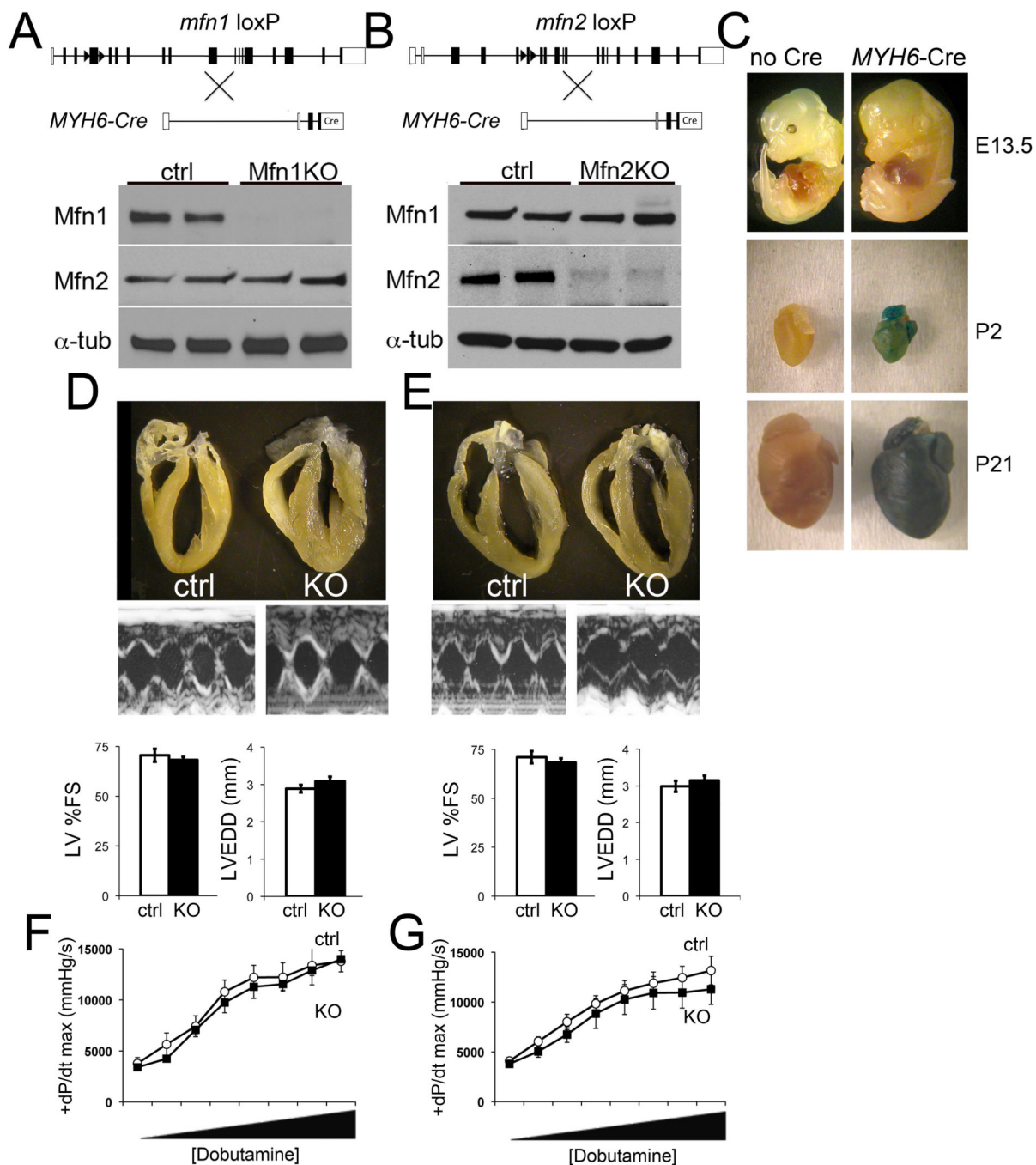


Figure 2. Postnatal heart-specific ablation of *Mfn1* and *Mfn2* using *Myh6*-directed nuclear-localized Cre

A. and **B.** Schematic representations of Cre-Lox strategy for cardiomyocyte-specific deletion of *mfn1* exon 4 and *mfn2* exon 6. Representative immunoblot analyses of cardiac *Mfn1* and *Mfn2* expression for each knockout (KO) is shown below; each column is a separate mouse heart. α -tub, α -tubulin loading control. **C.** Time of cardiomyocyte gene recombination by *Myh6*-nuclear-directed “turbo” Cre assessed by ROSA-26 LacZ reporter line. Recombination (blue staining) at 13.5 days p.c. (E13.5), the second day post birth (P2) and three weeks of age (P21). Top, whole embryos; middle and bottom, isolated hearts. Representative of at least four specimens per group. **D.** and **E.**, Representative hearts and M-

mode echocardiograms of mouse left ventricles. Group echocardiographic data are shown below (ctrl, white bars; Mfn KO, black bars; n=15–25 per group). LV %FS=left ventricular % fractional shortening; LVEDD=left ventricular end diastolic dimension. **F.** and **G.,** Invasive hemodynamic studies of cardiac contraction (peak rate of increase in LV pressure; +dP/dt max) and inotropic response to dobutamine-induced β_1 -adrenergic receptor stimulation. Dobutamine was infused intravenously at increasing doses from 4 to 256 ng/g/min. ctrl, white circles; Mfn KO, black squares. Data are of 3–5 per group.

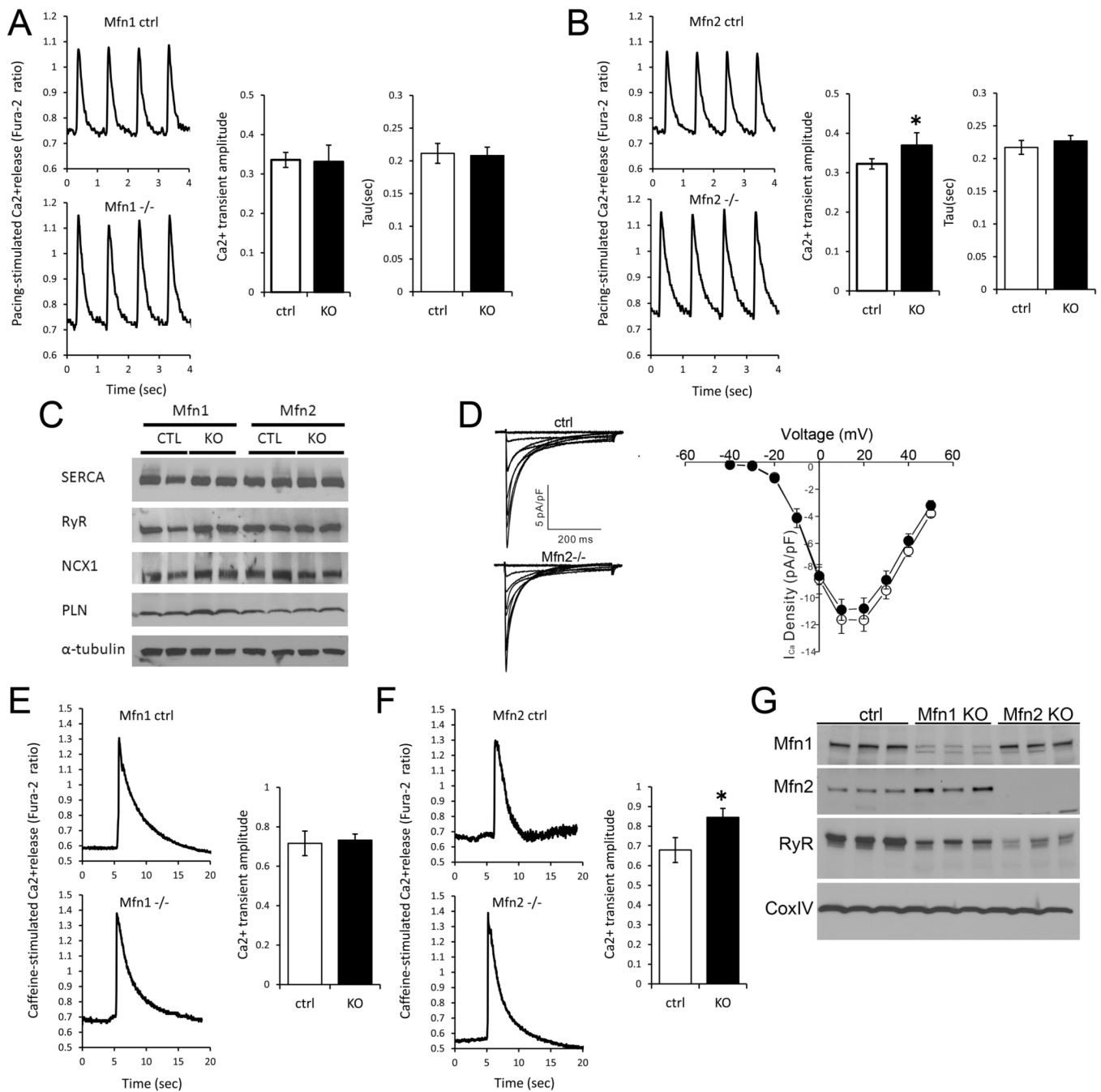


Figure 3. Ca²⁺ cycling and SR Ca²⁺ release in Mfn1 and Mfn1-deficient murine cardiac myocytes

A. and **B.**, Phasic Ca²⁺ transients in Fura-2 loaded field-stimulated isolated Mfn1- (A) and Mfn2 (B) null ventricular cardiac myocytes (-/-) and respective floxed allele controls (ctrl). Group quantitative data for transient amplitude and time constant for normalization (tau) are shown to the right. Data are averaged from n=5 paired hearts, averaging 8–12 cardiomyocytes per heart. **C.** Representative immunoblot analysis of SR calcium handling protein expression in Mfn1-/- and Mfn2-/- cardiac homogenates and their respective controls. SERCA=SR Ca²⁺-ATPase; RyR=ryanodine receptor 2; NCX1=Na⁺/Ca²⁺ exchanger; PLN=phospholamban. **D.** Representative whole-cell L-type Ca²⁺ currents

(normalized to cell capacitance), evoked in response to 400 ms depolarizing voltage steps to test potentials between -30 to $+50$ mV from a holding potential of -40 mV, recorded from control (CTL; *top*) and Mfn2 $^{-/-}$ (*bottom*) ventricular myocytes. Peak $I_{Ca,L}$ densities in CTL (n=11) and KO (n=16) LV myocytes are plotted as a function of the test potential on the right. **E.** and **F.** SR Ca^{2+} release by caffeine (10 mM) in isolated Mfn1 (**E**) and Mfn2 (**F**) null and control cardiac myocytes. Group data for Ca^{2+} signal amplitude are shown to the right. **G.** RyR content in mitochondrial-associated membranes from Mfn1 and Mfn2 KO mouse hearts. Cytochrome oxidase (Cox) is a mitochondrial protein loading control. *p<0.05 vs ctrl.

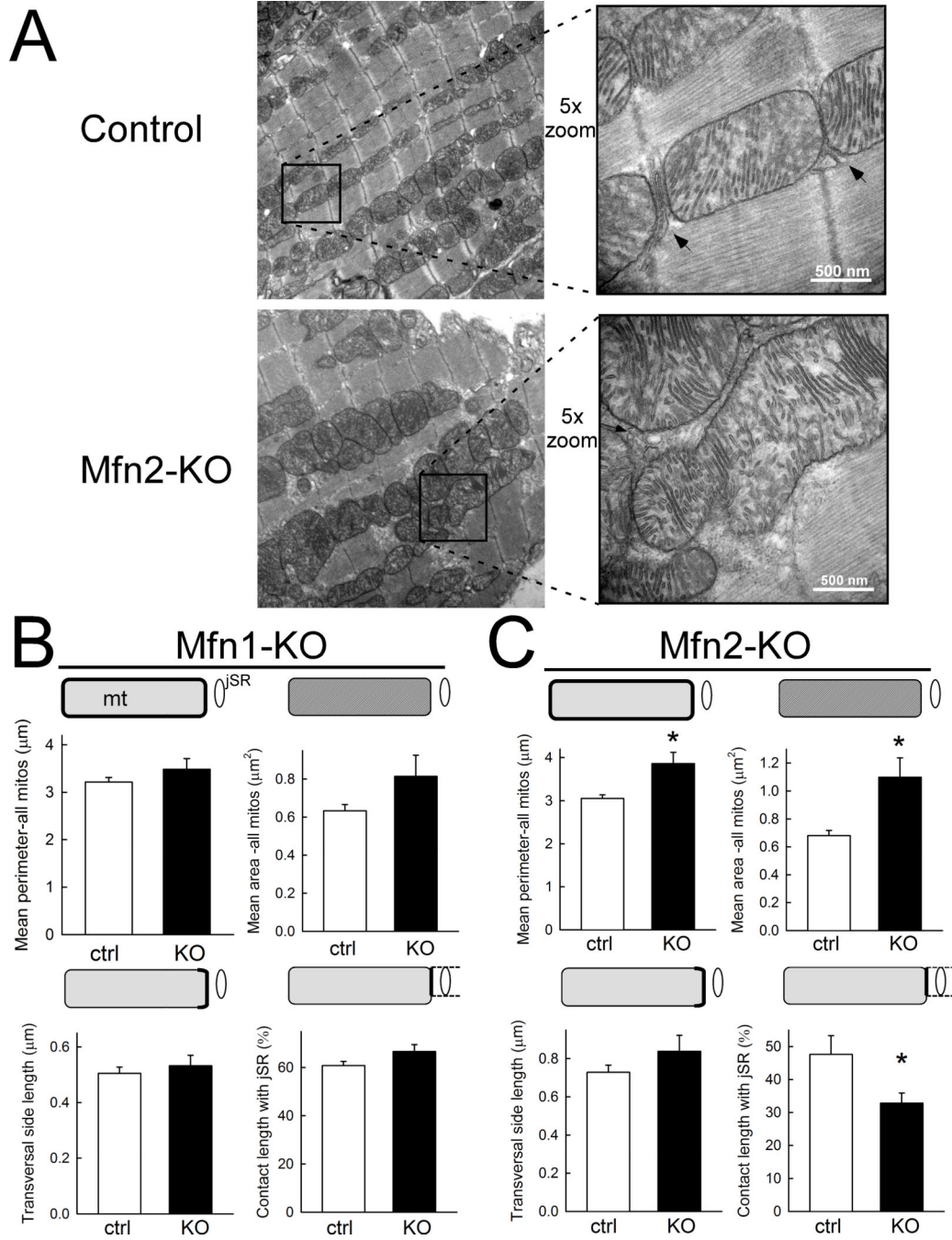


Figure 4. Cardiomyocyte mitochondrial-SR architecture is altered by Mfn2 ablation

A. Transmission electron micrographs of longitudinal sections of myocardium derived from control (top) and cardiac Mfn2-null (Mfn2-KO) mice (bottom). Lower magnification overview images on the left show the overall mitochondrial distribution and morphology. 5-fold higher magnification of the framed areas are shown on the right with arrows pointing to SR-mitochondrial associations. **B** and **C**, Cumulative analysis of mean perimeter (top, left) and area of mitochondria (top, right), and of the transverse side length (bottom, left) and contact length with jSR (bottom, right, respectively) in Mfn1- (**B**) and Mfn2-KO mice (**C**) compared to their respective controls. Mfn1-KO (**B**): n=8 and 6 cellular areas analyzed from

2 different hearts each for Mfn1-KO and control, respectively; each cellular area represents the means/sum of 117–377 and 144–299 individual mitochondria. Mfn2-KO (C): n=8 and 7 cellular areas from 4 different hearts each for Mfn2-KO and control, respectively; each cellular area represents the means/sum of 44–173 and 65–304 individual mitochondria. * $p < 0.05$ (Mann-Whitney rank sum test).

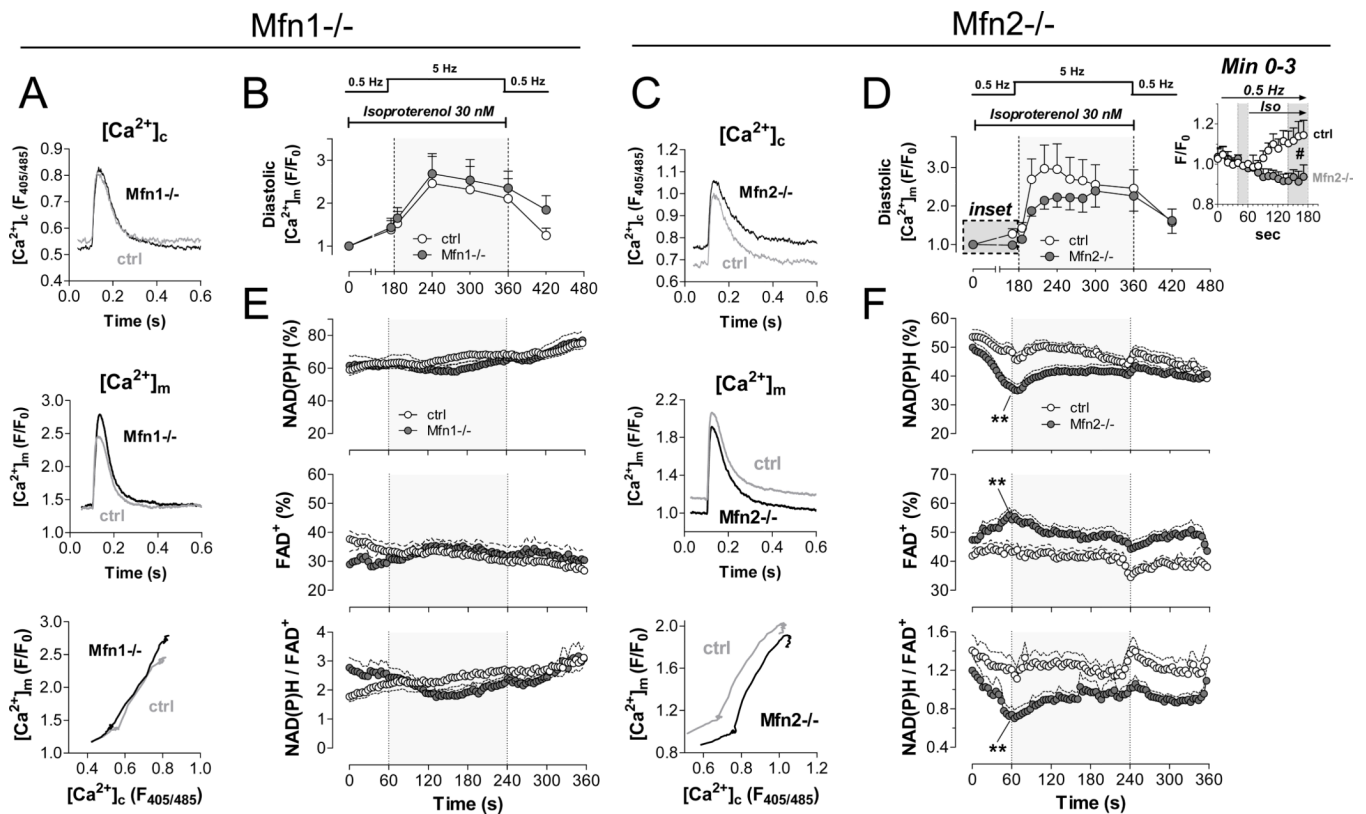


Figure 5. Impaired mitochondrial Ca^{2+} accumulation and bioenergetic feedback response in *Mfn2*-deficient myocytes

Experiments were performed on intact cardiac myocytes with acute isoproterenol and pacing stress (see Supplemental Figure 4); *Mfn1*-KO on left; *Mfn2*-KO on right. **A.** and **C.**

Averaged original traces of $[\text{Ca}^{2+}]_c$ (top) and $[\text{Ca}^{2+}]_m$ transients (middle) in WT and *Mfn*-KO myocytes after isoproterenol (30 nM) for 1 min at 0.5 Hz. *Bottom* panels show dynamic changes of $[\text{Ca}^{2+}]_m$ plotted against $[\text{Ca}^{2+}]_c$ in the same cell in the presence of isoproterenol for 1 min at 0.5 Hz (*Mfn1*: n=4 control, n=7 KO; *Mfn2*: n=14 control, n=12 KO).

B. and **D.** Time-dependent changes in diastolic $[\text{Ca}^{2+}]_m$ with pacing and isoproterenol stress. *Inset* in **D** shows change of diastolic $[\text{Ca}^{2+}]_m$ in the first 2 minutes after application of isoproterenol.

E. and **F.** Autofluorescence of NAD(P)H (top), FAD (middle) and the ratio of NAD(P)H/FAD (bottom; *Mfn1*-KO, n=17; control, n=7; *Mfn2*-KO, n=24; control, n=15). * $p < 0.05$ and ** $p < 0.01$ WT vs. KO, respectively (ANOVA for repeated measures).

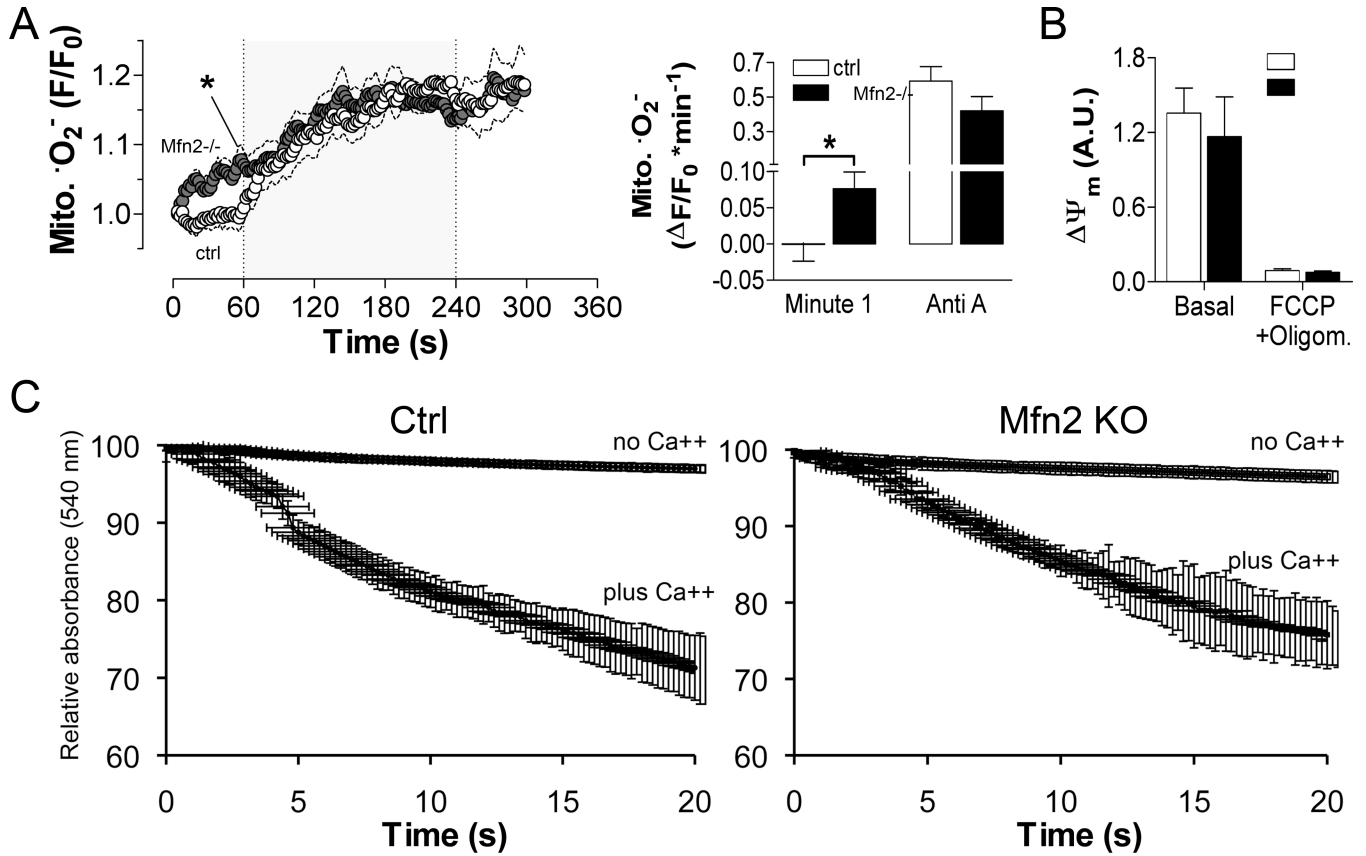


Figure 6. Effects of Mfn2 deletion on cardiomyocyte mitochondrial superoxide formation, $\Delta\Psi_m$ integrity and Ca^{2+} permeability

A. Superoxide ($\cdot O_2^-$) was measured using MitoSOX during studies performed as in Figure 5. *Left*, time-dependence of $\cdot O_2^-$ production; *right*, rate of mitochondrial $\cdot O_2^-$ production one minute after isoproterenol (Minute 1) and after antimycin A (Anti-A; n=16 ctrl, n=9 KO). **B.** Absolute fluorescence of TMRM indicating $\Delta\Psi_m$ at baseline and after mitochondrial uncoupling with FCCP (5 $\mu\text{mol/L}$) and oligomycin (1.26 $\mu\text{mol/L}$) in control and Mfn2-KO myocytes (n=10 WT, 4 KO). **C.** Ca^{2+} -induced swelling of isolated heart mitochondria was induced by addition of 250 μM $CaCl_2$ and quantified as the time-dependent decrease in absorbance at 540 nm. Results from ctrl are on the *left*, Mfn2 null on the *right*.